

# Single-molecule analysis of DNA uncoiling by a type II topoisomerase

Terence R. Strick, Vincent Croquette & David Bensimon

Laboratoire de Physique Statistique de l'Ecole Normale Supérieure, UMR 8550 CNRS, Universities of Paris VI and Paris VII, 24 rue Lhomond, 75231 Paris Cedex 05, France

Type II DNA topoisomerases are ubiquitous ATP-dependent enzymes capable of transporting a DNA through a transient double-strand break in a second DNA segment<sup>1</sup>. This enables them to untangle DNA<sup>2–6</sup> and relax the interwound supercoils (plectonemes) that arise in twisted DNA<sup>7</sup>. *In vivo*, they are responsible for untangling replicated chromosomes and their absence at mitosis or meiosis ultimately causes cell death<sup>8,9</sup>. Here we describe a micromanipulation experiment in which we follow in real time a single *Drosophila melanogaster* topoisomerase II acting on a linear DNA molecule which is mechanically stretched and supercoiled<sup>10–13</sup>. By monitoring the DNA's extension in the presence of ATP, we directly observe the relaxation of two supercoils during a single catalytic turnover. By controlling the force pulling on the molecule, we determine the variation of the reaction rate with the applied stress. Finally, in the absence of ATP, we observe the clamping of a DNA crossover by a single topoisomerase on at least two different timescales (configurations). These results show that single molecule experiments are a powerful new tool for the study of topoisomerases.

An un-nicked, double-stranded DNA molecule rigidly anchored at one end to a glass surface and at the other to a small magnetic bead can be stretched with a force  $F$  and twisted to a degree of supercoiling  $\sigma$  by translating and rotating small magnets above the sample<sup>10</sup>. These two mechanical parameters determine the molecule's extension  $l$ , which is monitored by measuring the three-dimensional position of the tethered bead (Fig. 1b). As one begins to rotate the magnets, the DNA's extension is unchanged and the torque increases linearly with the twist angle<sup>14</sup>. When a critical torque  $\Gamma_b \propto \sqrt{F}$  is reached<sup>14–16</sup> the molecule buckles (as would a twisted tube), forming a plectoneme and stabilizing the torque at its critical value. Thereafter it contracts regularly<sup>16</sup> (Fig. 1a) as

overwinding generates more supercoils<sup>11</sup>. The measured rate of contraction ( $\delta$ ) for DNA depends on  $F$  (for example, at  $F = 0.7$  pN we find  $\delta = 45$  nm per turn). At high force the torque in DNA can induce structural transitions before buckling occurs<sup>12,13</sup>, so these experiments were performed at low forces ( $F \leq 0.3$  pN for  $\sigma < 0$  and  $F \leq 5$  pN for  $\sigma > 0$ ).

Addition of topoisomerase (topo) II to the system results in an increase in  $l$  by an amount  $\delta(F)$  for every supercoil relaxed. In 10  $\mu$ M ATP, enzyme turnover is slow and relaxation is directly observed as stepwise events of size  $2\delta$  (Fig. 2a). This is expected for type II topoisomerases which are known to remove two DNA supercoils per cycle<sup>17</sup>. The single-exponential distribution of times between steps (Fig. 2b) is consistent with the use of one ATP per cycle<sup>18</sup>, although we cannot rule out the hydrolysis of a second ATP<sup>19,20</sup> on a timescale shorter than our temporal resolution of about 1 s.

As we increase the ATP concentration to 300  $\mu$ M, the turnover rate increases and individual steps in relaxation events—of total duration  $T_{\text{relax}}$ —are no longer resolved (Fig. 2c). If the time between relaxation events ( $T_{\text{wait}}$ ) is much greater than  $T_{\text{relax}}$ , we may assume that these events are due to a single topo acting processively. The probability of having two enzymes acting simultaneously is  $P(T_{\text{wait}} \cdot T_{\text{relax}} < \frac{T_{\text{relax}}}{T_{\text{wait}}}) \ll 1$  (assuming a Poisson process). The similarity of relaxation time traces is further evidence that we are observing single molecule events. Enzymatic removal of the approximately 30 supercoils typically present usually takes place in a single burst, indicating a processivity greater than 15 cycles.

Averaging these time traces yields the mean reaction time course at fixed concentration of ATP (300  $\mu$ M; Fig. 2d), which can be fit to a simple Michaelis–Menten model for the rate ( $\nu$ ) of disappearance of supercoils, that is, change in writhe ( $\Delta Wr$ ), such that  $\nu = V_0 \cdot \Delta Wr / (\Delta Wr + k_{1/2})$  with  $V_0 = 2.2$  cycles  $s^{-1}$  and  $k_{1/2} \approx 2$  supercoils. Similar results ( $k_{1/2} \approx 3$ ) can be deduced from bulk measurements<sup>7</sup>. However, our data clearly show that plectonemes are the enzymatic substrate. The enzyme is unable to relax supercoiled DNA efficiently below the buckling instability (data not shown).

To compare our results with known bulk data, we measured  $V_0$  as a function of ATP concentration at  $F = 0.7$  pN (Fig. 3a). Fitting this curve to a Michaelis–Menten model<sup>7</sup> for hydrolysis of ATP by topo II ( $V_0 = \frac{V_{\text{max}}[\text{ATP}]}{K_M + [\text{ATP}]}$ ) yields  $K_M = 270 \pm 40$   $\mu$ M and  $V_{\text{max}} = 3.6 \pm 0.2$  turnovers per second. These values are consistent with the data of ref. 7 ( $K_M = 280$   $\mu$ M,  $V_{\text{max}} \approx 1.5$  cycles  $sec^{-1}$ ). The higher rate measured here reflects the facts that (1) in

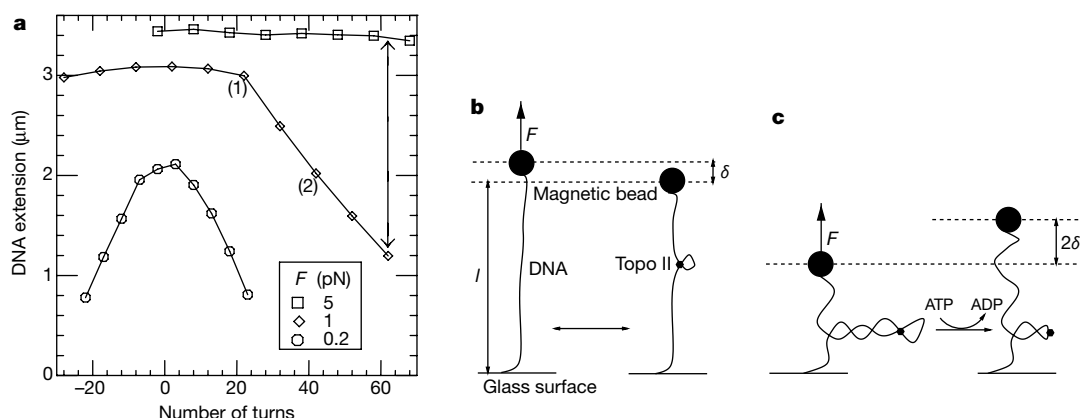


**Figure 1** Extension versus supercoiling behaviour for stretched DNA. **a**, At  $F = 1$  pN, the DNA needs to be overwound by about 25 turns before it reaches the buckling instability (point 1) and forms plectonemes. Thereafter the system contracts regularly (point 2). When underwound at this force however, DNA does not form plectonemes but locally denatures<sup>12</sup>. Increasing the force (arrow) on DNA overwound by 60 turns to 5 pN pulls out the plectonemes and causes the extension to increase. At  $F = 0.2$  pN the buckling instability is rounded off by thermal fluctuations but the DNA does not denature when

unwound. **b**, Sketch of a twisted DNA near the buckling instability (point 1 in **a**) undergoing topo II-mediated clamping in the absence of ATP. No supercoiling is relaxed, but stabilization and destabilization of a single DNA loop results in a change  $\delta$  of the system's extension. **c**, Supercoil relaxation in the plectonemic regime (point 2 in **a**) in the presence of topo II and ATP. Each enzymatic cycle releases two supercoils<sup>17</sup>, resulting in an increase  $2\delta$  of the system's extension.

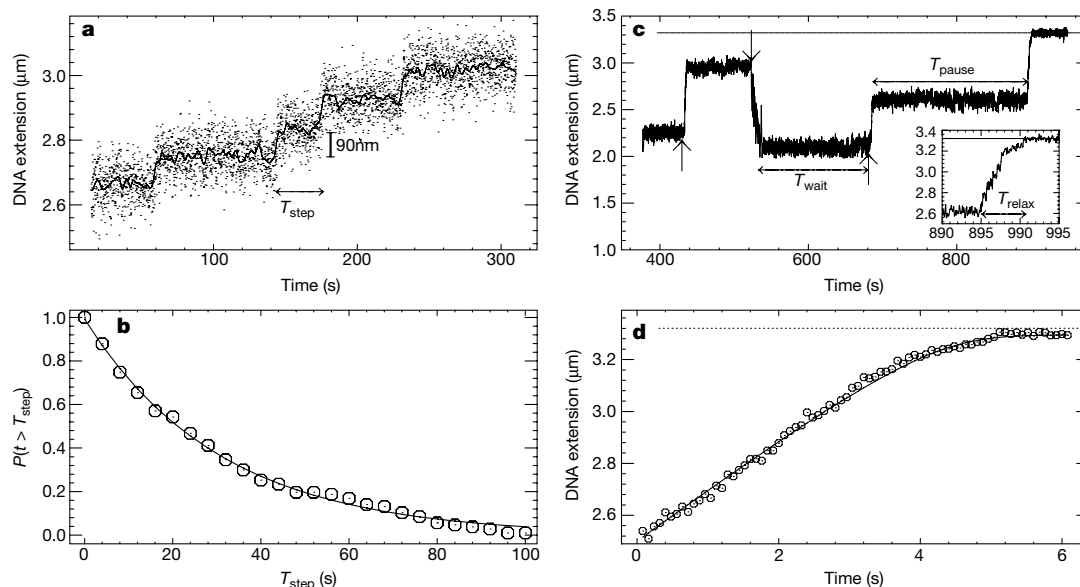


**Figure 2** Individual time courses for the topo II-mediated relaxation of positively supercoiled DNA stretched at  $F = 0.7$  pN. **a**, Individual steps in the system's extension ( $2\delta = 90$  nm  $\rightarrow \Delta Lk = 2$ ) can be observed at 10  $\mu$ M ATP. **b**, The cumulative distribution of time  $T_{\text{step}}$  between steps,  $P(t > T_{\text{step}})$ , displays a single-exponential behavior with  $\langle T_{\text{step}} \rangle = 28$  s. **c**, Mechanical overwinding of DNA (down arrow) followed by topo II-mediated relaxation (up arrow) at 300  $\mu$ M ATP. Interruptions in relaxation (pauses) may occur before  $Wr = 0$ , presumably due to the enzyme leaving its substrate, and are removed if  $T_{\text{pause}} > T_{\text{relax}}$ . Inset, an enlargement of the last relaxation curve in the panel.

bulk experiments the number of active enzymes is unknown and (2) our measurements do not include pauses in the enzyme's activity (Fig. 2b) nor the time spent searching for a DNA molecule.

To gain some insight into the reaction's kinetics, we also measured  $V_0$  as a function of  $F^{21,22}$  ( $0.3$  pN  $\leq F \leq 5$  pN) on positively supercoiled DNA in 1 mM ATP. Over this range of forces the turnover rate decreased by a factor of three (Fig. 3b), despite the fact that ATP was saturating (at  $F = 3$  pN the rates at [ATP] = 1 mM and [ATP] = 2 mM were identical within the error bars). It is surprising that raising the force (and thus the torque) acting on the DNA does not increase the reaction rate. Indeed, a larger force should facilitate opening of the DNA gate and a higher torque should decrease the barrier to strand passage. Instead our results imply that the enzyme is performing a work  $F \cdot \Delta$  (with  $\Delta \approx 1$  nm) against the force, with a consequent slowing down of its activity by an Arrhenius factor  $\exp(-F\Delta/k_B T)^{21}$ . This indicates that closure of the cleaved DNA segment may be rate-limiting. Finally, we found that the enzyme is nearly as efficient at relaxing negative or positive supercoils<sup>7</sup>,  $V_0^{\sigma < 0} = 2.6 \pm 0.2$  and  $V_0^{\sigma > 0} = 3.4 \pm 0.2$  turnovers per second respectively, ( $F = 0.3$  pN and [ATP] = 1 mM).

Although no strand transport occurs in the absence of ATP, previous experiments indicate that in these conditions the enzyme may still locate and stabilize a DNA supercoil by binding to a crossover between two DNA segments<sup>23,24</sup>. To verify the existence of such 'crossover clamping' events, we compare the stretching of positively supercoiled DNA ( $\sigma = 0.06$ ) subjected to a sudden increase in force (from  $F = 1$  pN to  $F = 5$  pN) in the absence or presence of enzyme (Fig. 4a, b). In the absence of enzyme, the force step causes the system's extension to increase smoothly as plectonemes are mechanically pulled out. In the presence of topo II, however, the bead's rise may be interrupted for a few seconds before abruptly resuming. The explanation for such abrupt events is that the enzyme has clamped a crossover between two DNA segments,

**d**, Data from 15 relaxation curves (each consisting of about 10 enzymatic turnovers) obtained at 300  $\mu$ M ATP are superimposed and averaged together after removal of pauses longer than 5 s. The continuous curve is a fit to a Michaelis-Menten equation for removal of the substrate ( $\Delta Wr = -\Delta l/\delta$ ) as a function of time  $t$ :  $\frac{d\Delta Wr}{dt} = -\frac{V_0 \Delta Wr}{\Delta Wr + k_{1/2}}$ , or  $k_{1/2} \log\left(\frac{l_{\text{max}} - l(t)}{l_{\text{max}} - l(0)}\right) + \frac{l(0) - l(t)}{\delta} = -V_0 t$  where  $l_{\text{max}}$  is the system's extension for  $Wr = 0$ ,  $l(0)$  its extension when relaxation begins at  $t = 0$ , and  $V_0$  and  $k_{1/2}$  are the reaction rate in cycles per second and the half-rate constant, respectively.

temporarily isolating a plectoneme. When the protein clamp releases, the plectoneme is subjected to the stretching force and is immediately pulled out, resulting in jumps in extension of up to about 0.6  $\mu$ m.

At a fixed force, supercoiling the DNA beyond the buckling instability favours the intermittent clamping of multiple plectonemes, which strongly alters the bead's Brownian fluctuations (data not shown). By reducing the degree of supercoiling, it becomes possible to measure individual clamping events directly. In the absence of topo II and at the threshold of the buckling instability ( $\sigma \approx 0.025$  for  $F = 1$  pN), a thermally excited loop may sporadically appear and disappear at a rate beyond the temporal resolution of

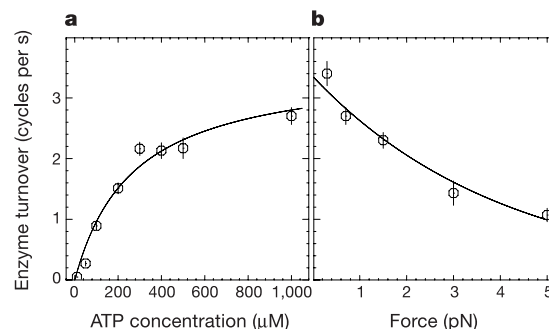


**Figure 3** Reaction dependence on ATP concentration and force. **a**, The maximal velocity  $V_0$  of the reaction at  $F = 0.7$  pN, determined from the initial slope of the averaged time courses (Fig. 2d), is plotted as a function of ATP concentration. Each point is an average over at least 100 enzymatic cycles. The continuous curve is a fit to a Michaelis-Menten model of enzyme kinetics (see text). **b**, Effect of the stretching force  $F$  on the velocity  $V_0$  measured at 1 mM ATP. The continuous curve is a fit to an Arrhenius dependence<sup>21</sup> where  $V_0 = V_0^{F=0} \exp(-F\Delta/k_B T)$  with  $\Delta \approx 1$  nm (see text). Error bars indicate the statistical error.

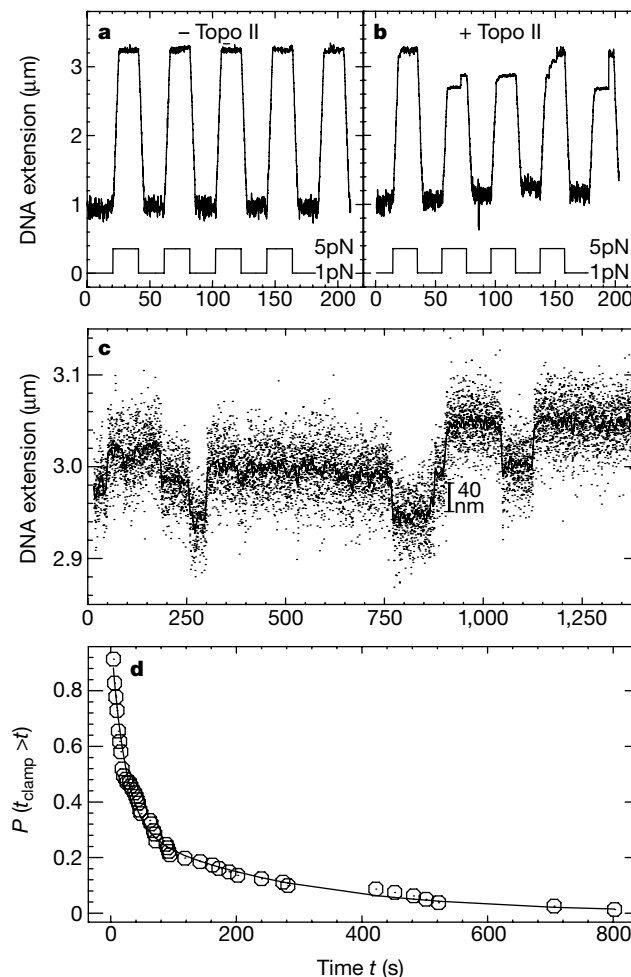


**Figure 4** Evidence for topo II clamping a crossover between two DNA segments (no ATP). **a, b**, Extension of positively supercoiled DNA ( $\sigma = 0.06$ ) subjected to an alternating force ( $F = 1$  pN or  $F = 5$  pN, bottom curves) in the absence (**a**) or presence (**b**) of enzyme. Sudden release of the protein clamp from a crossover allows the extension to rise abruptly (**b**, see text). **c**, Measurement of topo II/DNA clamping times at  $F = 1$  pN and  $\sigma = 0.025$ . Fixation of a DNA loop is characterized by a  $\delta \approx 40$  nm decrease in the system's extension; its release is detected when the system's extension increases by

the same length. Clamping times were measured when only one enzyme molecule was seen to interact with the DNA; here, multiple enzymes are seen to clamp multiple crossovers. **d**, The cumulative distribution of ninety clamping times is fit to a double-exponential behaviour characterized by two half-lives for the clamped states  $P(t_{\text{clamp}} > t) = \alpha \exp(-t/\tau_1) + (1 - \alpha) \exp(-t/\tau_2)$  with  $\alpha = 0.7$ ,  $\tau_1 = 20$  s and  $\tau_2 = 260$  s, and an error of about 10%.

our system. When topo II is introduced, the enzyme is seen to bind to and stabilize a loop (Fig. 1b) for times ranging from tens to hundreds of seconds. The system's extension decreases by  $\delta \approx 40$  nm until the enzyme lets go of the crossover (Fig. 4c). Measurement and analysis of these clamping events indicates that there are at least two distinct  $k_{\text{off}}$  rates for a topo II bound to a DNA crossover (Fig. 4d) as roughly 70% of the clamping events have a half-life of about 20 s, whereas the remaining 30% have a half-life of about 260 s. Whereas the long-lived clamping events are consistent with previous bulk experiments<sup>23,24</sup>, short-lived ones have not been observed before. They imply the existence of at least two different configurations for the enzyme/DNA–DNA complex in the absence of ATP.

We show that it is possible to observe the action of a single topo II as it uncoils a DNA molecule directly and in real time. Our results do not support the 'sliding-clamp' model for topo II<sup>6</sup>, which predicts a progressive increase in the DNA's extension upon supercoil removal. This model contradicts our observation of abrupt steps (Fig. 2a) and of decatenation of braided molecules under a  $F = 2$  pN load (data not shown). These experiments yield a wealth of quantitative data such as the off-rates of the enzyme from a DNA crossover and the behaviour under load of enzymatic rate. They may lead to a better characterization of the action of clinically-

relevant enzymatic inhibitors<sup>25</sup>. It will be interesting to extend this technique to the study of other related enzymes such as helicases and bacterial topo I, topo IV, gyrases and reverse gyrases. □

### Methods

We labelled 11-kilobase DNA (Charomid 9) at its extremities with biotin and digoxigenin as previously described<sup>12</sup> and bound it at one end to a streptavidin-coated magnetic bead (0.5  $\mu\text{m}$ , Merck). The bead–DNA construct was then incubated on an anti-digoxigenin-coated glass surface, previously incubated with BSA (Roche) to reduce non-specific interactions.

Relaxation experiments were performed at 25 °C in a 10 mM Tris buffer (pH 8) containing 100 mM NaCl, 50 mM KCl, 5 mM MgCl<sub>2</sub>, 0.1 mM EDTA, 0.2% Tween-20, 0.5 mM DTT and 200  $\mu\text{g ml}^{-1}$  BSA. DNA was mechanically wound to generate plectonemic supercoils, reducing the system's extension. Clamping experiments were performed<sup>24</sup> at 25 °C in a 50 mM Tris buffer (pH 8) containing 50 mM KCl, 8 mM MgCl<sub>2</sub>, 1 mM EDTA, 0.2% Tween-20, 0.5 mM DTT and 200  $\mu\text{g ml}^{-1}$  BSA. Topo II (Amersham and a gift from N. Cozzarelli) was at a final concentration of about 50 ng ml<sup>-1</sup>. ATP (Roche) was added to the final concentration indicated.

Bead tracking and force measurements were performed on an inverted microscope as previously described<sup>10</sup>. By tracking the three-dimensional position of the tethered bead<sup>12,13</sup> the extension  $l = \langle z \rangle$  of the molecule can be measured, with an error due to Brownian motion of about 10 nm with 1 s averaging. The bead's transverse fluctuations ( $\langle \delta x^2 \rangle$ ) allow a determination of the stretching force by the equipartition theorem where  $F = k_B T / \langle \delta x^2 \rangle$ . Here  $F$  has been measured with 10% accuracy. In plots showing the DNA's extension, the points presented are the raw data obtained at 12.5 Hz. When shown, solid lines correspond to data filtered at 1 Hz. To eliminate microscope drift, differential tracking with a second bead glued to the surface was performed.

Received 15 October 1999; accepted 10 February 2000.

1. Wang, J. C. Moving one DNA double helix through another by a type II DNA topoisomerase: the story of a simple molecular machine. *Q. Rev. Biophys.* **31**, 107–144 (1998).
2. Liu, L. F., Liu, C. C. & Alberts, B. M. Type II DNA topoisomerases: enzymes that can unknot a topologically knotted DNA molecule via a reversible double-stranded break. *Cell* **19**, 697–707 (1980).
3. Hsieh, T. Knotting of the circular duplex DNA by type II DNA topoisomerase from *D. melanogaster*. *J. Biol. Chem.* **258**, 8413–8420 (1983).
4. Roca, J. & Wang, J. C. The capture of a DNA double helix by an ATP-dependent protein clamp: a key step in DNA transport by type II DNA topoisomerase. *Cell* **71**, 833–840 (1992).
5. Roca, J., Berger, J. M. & Harrison, S. C. & Wang, J. C. DNA transport by a type II topoisomerase: Direct evidence for a two-gate mechanism. *Proc. Natl Acad. Sci. USA* **93**, 4057–4062 (1996).
6. Rybenkov, V. V., Ullsperger, C., Vologodskii, A. V. & Cozzarelli, N. R. Simplification of DNA topology below equilibrium values by type II topoisomerases. *Science* **277**, 690–693 (1997).
7. Osheroff, N., Shelton, E. R. & Brutlag, D. L. DNA topoisomerase II from *D. melanogaster*: relaxation of supercoiled DNA. *J. Biol. Chem.* **258**, 9536–9543 (1983).
8. Uemura, T. & Yanagida, M. Mitotic spindle pulls but fails to separate chromosomes in type II DNA topoisomerase mutants: uncoordinated mitosis. *EMBO J.* **5**, 1003–1010 (1986).
9. Ishida, R. *et al.* Inhibition of DNA topoisomerase II by ICRF-193 induces polyploidization by uncoupling chromosome dynamics from other cell cycle events. *J. Cell Biol.* **126**, 1341–1351 (1994).
10. Strick, T. R., Allemand, J. F., Bensimon, D., Bensimon, A. & Croquette, V. The elasticity of a single supercoiled DNA molecule. *Science* **271**, 1835–1837 (1996).
11. Strick, T. R., Allemand, J. F., Bensimon, D. & Croquette, V. The behavior of super-coiled DNA. *Biophys. J.* **74**, 2016–2028 (1998).
12. Strick, T. R., Croquette, V. & Bensimon, D. Homologous pairing in stretched supercoiled DNA. *Proc. Natl Acad. Sci. USA* **95**, 10579–10583 (1998).
13. Allemand, J. F., Bensimon, D., Lavery, R. & Croquette, V. Stretched and overwound DNA forms a Pauling-like structure with exposed bases. *Proc. Natl Acad. Sci. USA* **95**, 14152–14157 (1998).
14. Landau, L. & Lifschitz, E. *Theory of Elasticity* (Mir Editions, Moscow, 1967).
15. Moroz, J. D. & Nelson, P. Torsional directed walks, entropic elasticity and DNA twist stiffness. *Proc. Natl Acad. Sci. USA* **94**, 14418–14422 (1998).

## errata

### Uptake of apoptotic cells drives the growth of a pathogenic trypanosome in macrophages

Célio G. Freire-de-Lima, Danielle O. Nascimento, Milena B. P. Soares, Patricia T. Bozza, Hugo C. Castro-Faria-Neto, Fernando G. de Mello, George A. DosReis & Marcela F. Lopes

*Nature* **403**, 199–203 (2000)

In Fig. 4b and c the label beneath the fourth column should have read 'Apo-1 + indomethacin' rather than 'Anti- $\alpha_v$  + indomethacin'. □

### Formation of molecular gas in the tidal debris of violent galaxy–galaxy interactions

Jonathan Braine, Ute Lisenfeld, Pierre-Alain Duc & Stéphane Leon

*Nature* **403**, 867–869 (2000)

The name of the third author, Pierre-Alain Duc, was inadvertently mis-spelled as Due. In Fig. 3, the right-hand vertical axis label should have been the same as that for the left-hand vertical axis: 'CO(1  $\rightarrow$  0) temperature (mK)'. □

16. Bouchiat, C. & Mézard, M. Elasticity model of a supercoiled DNA molecule. *Phys. Rev. Lett.* **80**, 1556–1559 (1998).
17. Brown, P. O. & Cozzarelli, N. R. A sign inversion mechanism for enzymatic supercoiling of DNA. *Science* **206**, 1081–1083 (1979).
18. Hua, W., Young, E. C., Fleming, M. L. & Gelles, J. Coupling of kinesin steps to ATP hydrolysis. *Nature* **388**, 390–393 (1997).
19. Harkins, T. T. & Lindsley, J. E. Pre-steady-state analysis of ATP hydrolysis by *Saccharomyces cerevisiae* DNA topoisomerase II. 1. A DNA-dependent burst in ATP hydrolysis. *Biochemistry* **37**, 7292–7298 (1998).
20. Harkins, T. T., Lewis, T. J. & Lindsley, J. E. Pre-steady-state analysis of ATP hydrolysis by *Saccharomyces cerevisiae* DNA topoisomerase II. 2. Kinetic mechanism for the sequential hydrolysis of two ATP. *Biochemistry* **37**, 7299–7312 (1998).
21. Wang, M. D. *et al.* Force and velocity measured for single molecules of RNA polymerase. *Science* **282**, 902–907 (1998).
22. Visscher, K., Schnitzer, M. J. & Block, S. M. Single kinesin molecules studied with a molecular force clamp. *Nature* **400**, 184–189 (1999).
23. Zechiedrich, E. L. & Osheroff, N. Eukaryotic topoisomerases recognize nucleic acid topology by preferentially interacting with DNA crossovers. *EMBO J.* **9**, 4555–4562 (1990).
24. Roca, J., Berger, J. M. & Wang, J. C. On the simultaneous binding of eukaryotic DNA topoisomerase II to a pair of double-stranded DNA helices. *J. Biol. Chem.* **268**, 14250–14255 (1993).
25. Froelich-Ammon, S. J. & Osheroff, N. Topoisomerase poisons: harnessing the dark side of enzyme mechanism. *J. Biol. Chem.* **270**, 21429–21432 (1995).

## Acknowledgements

We thank B. Maier and J.-F. Allemand for helpful comments and O. Hyrien, J.-L. Sikorav, M. Duguet, V. Rybenkov, N. Crisona and N. Cozzarelli for stimulating conversations. We also thank N. Cozzarelli for a gift of cloned topo II. T.R.S. was supported by a CNRS BDI fellowship.

Correspondence and requests for materials should be addressed to T.R.S. or D.B.

## corrections

### The DNA sequence of human chromosome 22

I. Dunham, N. Shimizu, B. A. Roe, S. Chisoe *et al.*

*Nature* **402**, 489–495 (1999)

The names of the following authors were omitted from the complete list at the end of the Article: P. Wilkinson (The Sanger Centre, Wellcome Trust Genome Campus, Hinxton, Cambridge CB10 1SA, UK); A. Bodenteich, K. Hartman, X. Hu, A. S. Khan, L. Lane, Y. Tilahun & H. Wright (Department of Chemistry and Biochemistry, The University of Oklahoma, 620 Parrington Oval, Room 311, Norman, Oklahoma 73019, USA). □

### Tribosphenic mammal from the North American Early Cretaceous

Richard L. Cifelli

*Nature* **401**, 363–366 (1999)

The binomen *Montanalestes keebleri* was established for a tribosphenic mammal of probable eutherian affinities from the Lower Cretaceous (Aptian–Albian) Cloverly Formation, Montana, USA. The trivial name was designated for the Keebler family, of Billings, Montana. As pointed out to me by T. Harrison, this designation is implicitly plural, hence, the proper suffix is *-orum*<sup>1</sup>. The species name is hereby corrected to *Montanalestes keeblerorum*, as provided by articles 19 and 32 of the International Code of Zoological Nomenclature<sup>1</sup>. □

1. International Commission on Zoological Nomenclature. *International Code of Zoological Nomenclature* 4th edn (International Trust for Zoological Nomenclature, The Natural History Museum, London, 1999).